Talanta 207 (2020) 120321

Contents lists available at ScienceDirect

Talanta

journal homepage: www.elsevier.com/locate/talanta

Reflectance aptasensor based on metal salphen label for rapid and facile determination of insulin

Mahirah Taib[a], Ling Ling Tan[a,*], Nurul Huda Abd Karim[b], Goh Choo Ta[a], Lee Yook Heng[a,b], Bahariah Khalid[c,d]

[a] Southeast Asia Disaster Prevention Research Initiative (SEADPRI-UKM), Institute for Environment and Development (LESTARI), Universiti Kebangsaan Malaysia, 43600, UKM Bangi, Selangor Darul Ehsan, Malaysia
[b] School of Chemical Sciences and Food Technology, Faculty of Science and Technology, Universiti Kebangsaan Malaysia, 43600, UKM Bangi, Selangor Darul Ehsan, Malaysia
[c] Department of Medicine, Faculty of Medicine and Health Sciences, Universiti Putra Malaysia, 43400, UPM Serdang, Selangor Darul Ehsan, Malaysia
[d] Hospital Serdang, Jalan Puchong, 43000, Kajang, Selangor Darul Ehsan, Malaysia

ARTICLE INFO

Keywords:
Aptasensor
DNA aptamer
Insulin
Metal salphen label
Visual detection

ABSTRACT

An optical aptasensor-based sensing platform for rapid insulin detection was fabricated. Aminated porous silica microparticles (PSiMPs) were synthesized via a facile mini-emulsion method to provide large surface area for covalent immobilization of insulin-binding DNA aptamer (IGA3) by glutaraldehyde cross-linking protocol. A Nickel-salphen type complex with piperidine side chain [Ni(II)-SP] was synthesized with a simple one-pot reaction, and functionalized as an optical label due to strong π-π interaction between aromatic carbons of G-quadruplex DNA aptamer and planar aromatic groups of Ni(II)-SP to form the immobilized IGA3-Ni(II)-SP complex, i.e. the dye-labeled aptamer, thereby bringing yellow colouration to the immobilized G-quartet plane. Optical characterization of aptasensor towards insulin binding was carried out with a fiber optic reflectance spectrophotometer. The maximum reflectance intensity of the immobilized IGA3-Ni(II)-SP complex at 656 nm decreased upon binding with insulin as aptasensor changed to brownish orange colouration in the background. This allows optical detection of insulin as the colour change of aptasensor is dependent on the insulin concentration. The linear detection range of the aptasensor is obtained from 10 to 50 μIU mL^{-1} (R^2 = 0.9757), which conformed to the normal fasting insulin levels in human with a limit of detection (LOD) at 3.71 μIU mL^{-1}. The aptasensor showed fast response time of 40 min and long shelf life stability of > 3 weeks. Insulin detection using healthy human serums with informed consent provided by participants suggests the DNA aptamer biosensor was in good agreement with ELISA standard method using BIOMATIK Human INS (Insulin) ELISA Kit.

1. Introduction

Insulin is a peptide hormone secreted by beta cells in the pancreatic islet of Langerhans. Insulin molecule consists of two polypeptide interchains grafted by two disulphide bonds, of which A chain is made up of 21 amino acids and B chain of 30 amino acid residues. The main function of insulin is to maintain normal blood glucose levels in the body via regulating carbohydrate, protein and lipid metabolisms as well as promoting cell division and growth through its mitogenic effects [1]. The normal fasting blood serum insulin levels is lesser than 30 μIU mL^{-1} [2]. A high level of fasting insulin would indicate insulin resistance and prediabetes when the body does not use insulin well, whilst the failure of pancreas to produce sufficient insulin or any insulin at all, or the failure of body's cells to make proper use of insulin that is produced can lead to diseases such as diabetes, insulinoma and insulin resistance [3]. Therefore, insulin detection is of paramount importance for clinical diagnosis as it could serve as a predictor of diabetes-associated diseases.

Enzyme-linked immunosorbent assay (ELISA), radioimmunoassay (RIA), immunoradiometric assay (IRMA) and high performance liquid chromatography (HPLC) are the conventional methods for insulin determination [4]. Although they provide accurate and reliable results but they require cumbersome and sophisticated instruments, radioactive reagent, high operational costs, technical expertise and time consuming, which limits their usage for real time *in situ* applications [5]. In recent years, there has been intensive research to determine insulin

* Corresponding author.
E-mail addresses: mahirahtaib17@gmail.com (M. Taib), lingling@ukm.edu.my, babybabeoo@gmail.com (L.L. Tan), nurulhuda@ukm.edu.my (N.H. Abd Karim), gohchoota@ukm.edu.my (G.C. Ta), leeyokheng@yahoo.co.uk (L.Y. Heng), bahariah@upm.edu.my (B. Khalid).

https://doi.org/10.1016/j.talanta.2019.120321
Received 19 July 2019; Received in revised form 1 September 2019; Accepted 3 September 2019
Available online 09 September 2019
0039-9140/

using electrochemical methods based on various types of advanced materials modified electrodes e.g. noble metals, metal oxide, silica nanoparticles, carbon nanotubes and multiwalled carbon nanotubes [6–9]. However, these electrodes sustained poor long term stability and long assay time due to slow oxidation kinetics [7].

Despite of the wide availability of enzymes and antibodies are utilized as recognition elements of biosensor, but they are heat- and acid-labile. In contrast, DNA can withstand heat and extreme conditions more than protein molecules, therefore DNA aptamer can act as ideal alternative recognition element in the biosensor configuration [6]. Nucleic acid aptamer is an artificial single stranded oligonucleotide selected from a large pool of random sequences through *in vitro* selection method referred to as systematic evolution of ligands by exponential enrichment (SELEX). DNA aptamers can bind specifically to their targets in the same manner as that of antibodies but with higher affinity for their targets and smaller in size compared to antibodies. DNA aptamers change their conformation when interact with target analyte. They can exhibit as G-quadruplexes, pseudoknots or hairpin-loops [10]. By merging the versatility of advanced micro/nanomaterials and DNA aptamers' capabilities, it has opened a new assortment of biosensor platforms for ultra-high sensitivity and selectivity detection of a wide variety of target compounds ranging from organic dyes, peptides, protein, heavy metal and bacteria cells [10,11].

Metal salphen complex is a Schiff base derivative that consists of azomethine or imine group (-HC═N-). The development of small-molecule-based Schiff base ligands and their transition metal complexes revealed a number of different binding modes to DNA e.g. groove binding, electrostatic interaction and intercalation of planar ligand complex in the DNA base pairs stack through non-covalent π-π stacking [12,13]. Previous binding study conducted by Georgiades et al. [14] have found that metal salphen complexes shown exceptional high affinity binding towards G-quadruplex DNA, and the addition of side chain or substituent group such as alkylamine could increase the solubility of metal salphen ligands in the aqueous solution [15], which holds great promise for a variety of applications including biosensing purposes.

Herein, we report the construction of an optical DNA aptamer biosensor based on metal salphen label that allows visual detection of insulin with reflectance transducer. Insulin-binding DNA aptamer (IGA3) was employed as the synthetic receptor and conjugated to the amine modified porous silica microparticles (PSiMPs) via imine covalent bonds using glutaraldehyde crosslinker. The IGA3 aptamer is a guanine (G)-rich DNA aptamer that forms an anti-parallel G-quadruplex and binds insulin selectively. Nickel(II) salphen, a Schiff base complex modified with piperidine side chain [NI(II)-SP] was acted as ligand to the immobilized DNA aptamer via non-covalent π-π stacking between aromatic rings of folded single strand IGA3 aptamer and square planar salphen ligand. The aptasensor demonstrated a colour change from yellow to brownish orange as the immobilized IGA3-Ni(II)SP complex bound with insulin, and a substantial decrement in the optical reflectance response can be measured with a fiber optic reflectance spectrophotometer. Fig. 1 illustrates the schematic diagram of step-wise fabrication of DNA aptamer biosensor for optical determination of insulin.

2. Experimental

2.1. Instrumentation

Attenuated Total Reflectance (ATR) result was acquired from Agilent Cary 630 FTIR spectrometer. 1-dimensional (1D) and 2-dimensional (2D) Nuclear Magnetic Resonance (NMR) spectra were recorded on a Bruker Avance III (400 MHz) NMR spectrometer using tetramethyl silane (TMS) as an internal standard and deuterated chloroform ($CDCl_3$-d) as a solvent. Mass spectra were obtained from BRUKER MicroTof-Q with DIONEX Ultimate 3000 LC. Field emission scanning electron microscopy (FESEM) was used to examine the size and morphology of porous silica microparticles (PSiMPs). The particle size and zeta potential of the as-synthesized PSiMPs were measured by zetasizer (Malvern). X-ray diffraction pattern of PSiMPs was captured at room temperature (25 °C) on Bruker's D8 Advanced Diffractometer. Reflectance response of the aptasensor was visualized using a reflectance spectrometer (SD 2000 Ocean Optics) coupled with bifurcated optical fiber probe, and DH-2000-BAL UV-VIS-NIR light source in the wavelength range of 200–1099 nm.

2.2. Chemicals and reagents

Tetraethyl orthosilicate (TEOS, 98%) and Tween 20 surfactant were supplied by Fluka. Glutaraldehyde (50%), 3-aminopropyltriethoxysilane (APTES, 98%), 1-(2-chloroethyl)piperidine hydrochloride, 2,5-dihydroxybenzaldehyde, Nickel(II) acetate tetrahydrate [$Ni(OCOCH_3)_2{\cdot}4H_2O$], potassium carbonate ($K_2CO_3$), C-reactive protein from human fluids and bovine serum albumin (BSA) were obtained from Sigma-Aldrich. Sodium fluoride, ethanol (EtOH, 98%), *N,N′*- dimethylformamide (DMF) and diethyl ether were purchased from R&M chemicals. Dimethyl sulfoxide, chloroform and *o*-phenylenediamine (98%) were procured from Merck, Acros Organics and J.T. Baker, respectively. The aptamer against insulin used in this work, i.e. IGA3 with amino modifier positioned at the 5′-end at a standard C6 spacer arm (5′-AmC6-GGT GGT GGG GGG GGT TGG TAG GGT GTC TTC-3′) was supplied by Sigma-Aldrich. Insulin solution from bovine pancreas was obtained from Sigma. TKN buffer solution was prepared from 50 mM Tris-HCl, 10 mM KCl and 100 mM NaCl at pH 7.4 as described by Yoshida et al. [16]. 20 μM IGA3 aptamer and 1000 μIU mL^{-1} bovine pancreas insulin stock solutions were prepared in TKN buffer solution at pH 7.4, and kept in the refrigerator at 4 °C.

2.3. Synthesis of piperidine functionalized nickel(II) salphen complex

Nickel(II) salphen complex with piperidine side chain [Ni(II)-SP] was synthesized according to the previously reported methods [17,18] with slight modifications. N,N′-bis-5-(hydroxysalicylidene)phenylenediamine-nickel(II) complex was first synthesized by reacting 0.69 g of 2,5-dihydroxybenzaldehyde (5 mmol) with 0.27 g of *o*-phenylenediamine (2.5 mmol) in 40 mL EtOH solution. The mixture was refluxed at 70 °C for 30 min prior to the addition of 1.244 g of $Ni(OCOCH_3)_2{\cdot}4H_2O$ (5 mmol), and the mixture was refluxed for another 4 h [Eq. (1)]. The resulting precipitation was then thoroughly washed by decantation using 50 mL of EtOH followed by 50 mL of deionized water and 50 mL of diethyl ether. The resultant product obtained at 0.3969 g of nickel(II) salphen complex (0.98 mmol) was reacted with 1.084 g of K_2CO_3 (7.84 mmol) and 0.7234 g of 1-(2-chloroethyl)piperidine in 60 mL of DMF solvent before undergoing another reflux procedure at 90 °C for 72 h [Eq. (2)]. The final yield was filtered off and evaporated on a rotary evaporator to remove DMF solvent before it was washed with deionized water and dried in a desiccator. The stock solution of Ni(II)-SP complex at 5 mM was prepared by dissolving 4.7 mg of the metal salphen complex in 1500 μL of DMSO solution. Dilution of the Ni(II)-SP complex to 1 mM was done using TKN buffer solution (pH 7.4).

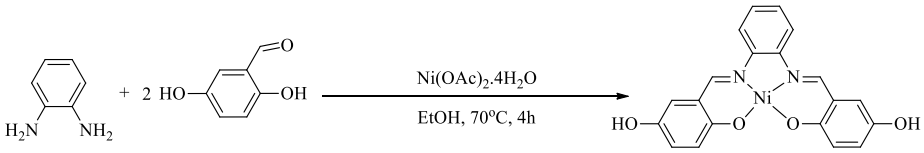

(1)

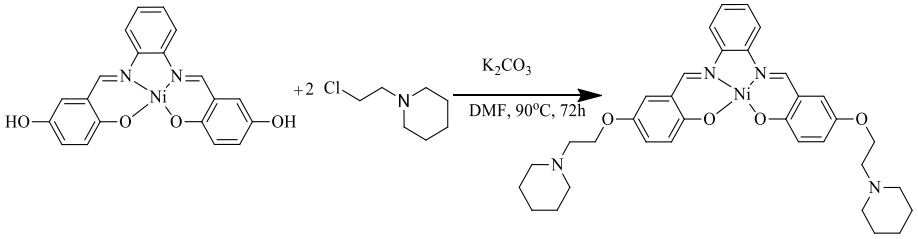

(2)

2.4. Synthesis of aminated porous silica particles

Aminated porous silica particles (PSiMPs) was synthesized based on our previously reported method [19] with some modifications. In brief, some 45 mL of TEOS was mixed with 20 mL of Tween 20 surfactant on a magnetic stirrer for 20 min. The mixture was then added dropwise into 20 mL of deionized water in the presence of 2 mL of APTES and 0.74 g of sodium fluoride (NaF, 0.0176 mol) catalyst before sonicated for 2 h. The resulting emulsion suspension was incubated for 24 h at ambient temperature in an incubator shaker. The white precipitate was later centrifuged at 400 rpm for 15 min, and sequentially washed with abundant EtOH and deionized water. After that, the white slurry formed was dried and calcined using furnace at 200 °C for 6 h followed by 600 °C for another 6 h 2 mL aliquot of APTES was added to the silica particles and stirred overnight using magnetic stirrer. 50 mg of the as-prepared aminated porous silica was finally suspended in 500 µL of EtOH before further usage.

2.5. Fabrication of optical insulin aptasensor

120 µL of aminated PSiMPs (50 mg/500 µL ethanol) was first deposited in the Eppendorf tube's cap of diameter 4 mm, and left to dry overnight at room temperature. 120 µL of glutaraldehyde was then added to the amine modified porous silica particles, and left for an hour at ambient conditions to activate the amine functional groups followed by washing with copious amount of TKN buffer at 7.4 to remove the excess glutaraldehyde cross-linkers on the PSiMPs surface. About 45 µL of 4 µM IGA3 aptamer was annealed for 5 min at 90 °C on a heating block, and 4.8 µL of the annealed DNA aptamer was dispensed on the glutaraldehyde modified PSiMPs to allow covalent binding to take place over a 24-h period. TKN buffer solution was later used to remove the excess DNA aptamer. 32 µL of 1 mM Ni(II)-SP label and 24 µL of insulin are then simultaneously deposited on the aptasensor micro surface and left for 40 min. The insulin aptasensor was rinsed with a plentiful amounts of TKN buffer solution at pH 7.4 prior to reflectance measurement using an optical fiber reflectance spectrophotometer.

2.6. Optimizing the reflectance DNA aptamer biosensor for insulin detection

2.6.1. Buffer and pH optimizations

Three types of buffer solutions were used to examine the reflectance response of aptasensor against the determination of 50 µIU mL^{-1} insulin in the presence of 1 mM Ni(II)-SP complex at pH 7.4 i.e. TKN buffer, phosphate buffer saline (PBS) and sodium phosphate buffer (NPS). TKN buffer was prepared by mixing 50 mM Tris-HCl, 10 mM KCl and 100 mM NaCl, and hydrochloric acid (HCl) was added dropwise until it reached at pH 7.4. PBS buffer was prepared by mixing 0.137 M sodium chloride (NaCl), 2.7 mM potassium chloride (KCl), 0.01 M disodium hydrogen phosphate (Na_2HPO_4) and 1.8 mM potassium dihydrogen phosphate (KH_2PO_4), and the solution pH was adjusted to pH 7.4.0.05 M NPS buffer at pH 7.4 was prepared by adding 0.05 M NaH_2PO_4 to 0.05 M Na_2HPO_4 until desired pH was reached at pH 7.4. pH optimization of the insulin aptasensor was carried out by preparing a series of TKN buffer solutions containing 50 µIU mL^{-1} insulin at pH 6.0, pH 6.4, pH 7.0, pH 7.4 and pH 8.0, and the aptasensor optical response was recorded at 656 nm in the presence of 1 mM Ni(II)-SP label.

2.6.2. Evaluation of aptasensor optical response towards different insulin concentrations

The optical response of the aptasensor towards different insulin concentrations was performed by preparing a series of bovine pancreas insulin solutions from 1 to 200 µIU mL^{-1} in TKN buffer containing 1 mM Ni(II)-SP Schiff base ligand at pH 7.4, and the reflectance

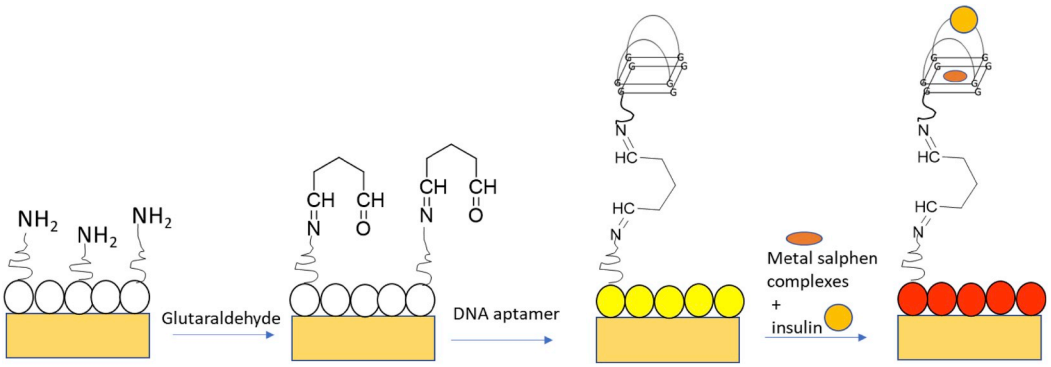

Fig. 1. Schematic representation of the step-wise fabrication of optical insulin aptasensor based on IGA3 G-quadruplex DNA aptamer modified PSiMPs supporting matrix and Ni(II)-SP label.

response was evaluated at 656 nm. The response curve of the optical aptasensor was then plotted between 1 μIU mL^{-1} and 200 μIU mL^{-1} insulin. A dynamic linear concentration range of the insulin aptasensor was established using linear trendline, and the linearity of dynamic response curve was estimated based on the linear correlation coefficient (R^2) value.

2.6.3. Regeneration and selectivity studies

Regeneration study was conducted by depositing 1 mM Ni(II)-SP label and 50 μIU mL^{-1} insulin on the aptasensor surface, and allowed to react for 40 min before it was washed with abundant TKN buffer (pH 7.4) followed by reflectance measurement of the aptasensor at 656 nm. The aptasensor was then thoroughly washed with 0.1 M sodium hydroxide (NaOH) regeneration solution, and immersed in 0.1 M NaOH for 5 min 1 mM Ni(II)-SP Schiff base complex and 50 μIU mL^{-1} insulin were added again on the aptasensor surface, and left for 40 min before another reflectance response was taken at 656 nm. This procedure was repeated until a significant decline in the reflectance intensity of the aptasensor was observed at 656 nm. As for aptasensor selectivity study, five different types of substances, such as ascorbic acid, bovine serum albumin (BSA), C-reactive peptide, D+ glucose monohydrate and uric acid were prepared separately in TKN buffer (pH 7.4) at physiological concentrations normally present in human blood serum, i.e. 0.0568 mM, 0.6018 mM, 2.5×10^{-6} mM, 4 mM and 0.1785 mM, respectively. Selectivity study was done based on separate solution method (SSM), whereby optical response of the aptasensor towards ascorbic acid, BSA protein, C-reactive protein, D+ glucose monohydrate and uric acid at 656 nm were evaluated separately in the present of 1 mM Ni(II)-SP compound, and compared with the aptasensor reflectance response against 50 μIU mL^{-1} insulin at 656 nm.

2.6.4. Aptasensor response time and long term stability studies

The response time of aptasensor was determined by measuring the aptasensor reflectance response at 656 nm every 10 min during the determination of 50 μIU mL^{-1} insulin in TKN buffer at pH 7.4 until 60 min. To determine the shelf life of reflectance aptasensor, 180 units of aptasensors were made from the same batch of materials, and stored at ambient conditions in several petri dishes when not in use. 3 units of aptasensors were tested with 50 μIU mL^{-1} insulin and 1 mM Ni(II)-SP complex in TKN buffer (pH 7.4) at different days within a 50-day of experimental period, and the reflectance response at 656 nm was captured during the course of the experiment.

2.7. Recovery test

Recovery test was done using commercial insulin obtained from a pharmaceutical company. Some 500 μL of commercial insulin was diluted with TKN buffer (pH 7.4) in a 50 mL volumetric flask, and dispensed into 4 units of 10 mL volumetric flasks. Known amount of standard bovine pancreas insulin at 20 μIU mL^{-1}, 30 μIU mL^{-1}, 40 μIU mL^{-1} and 50 μIU mL^{-1} were then spiked into the respective diluted commercial insulin samples, and the flasks were carefully topped up to the graduation mark of the respective flasks with diluted commercial insulin at pH 7.4.32 μL of 1 mM Ni(II)-SP Schiff base label and 24 μL of spiked insulin sample were deposited on the aptasensor surface, and optical signal at 656 nm was monitored with fiber optic reflectance spectrophotometer after 40 min of reaction time.

2.8. Validation of aptasensor with ELISA kit for insulin detection

Three identified healthy volunteers had provided informed consent for the collection and usage of their samples for insulin assay with developed aptasensor and validation with ELISA standard method. 18 mL of blood sample was collected into 3 plain red-top VACUTAINER® tubes for each healthy volunteer, and allowed to clot for 20 min at room temperature before centrifugation for 15 min in a refrigerated centrifuge at 1000 × *g* and 6 °C. The supernatant was then collected to carry out the assay with both aptasensor and BIOMATIK Human INS (Insulin) ELISA Kit. The ELISA kit uses the sandwich-ELISA principle. The micro ELISA plate provided in this kit has been pre-coated with an antibody specific to insulin. The samples at 100 μL each were added to the micro ELISA plate wells and combined with the specific antibody. Then, 100 μL of biotinylated detection antibody specific towards insulin and avidin-horseradish peroxidase (HRP) conjugate were added successively to each micro plate well and incubated at 37 °C for 30 min. Free components were washed away with wash buffer for 5 times followed by adding 90 μL of substrate reagent to each well. Only those wells that contain insulin, biotinylated detection antibody and avidin-HRP conjugate appeared blue in colour. The enzyme substrate reaction was terminated by the addition of 50 μL stop solution and the colour turned yellow. The optical density (OD) was measured spectrophotometrically at a wavelength of 450 ± 2 nm. The OD value is proportional to the concentration of insulin. As for insulin level assayed by optical aptasensor, 32 μL of 1 mM Ni(II)-SP label and 24 μL of serum sample were deposited on the fabricated aptasensor surface, and left for 40 min prior to rinsing with TKN buffer (pH 7.4) and reflectance measurement with fiber optic reflectance spectrophotometer.

3. Results and discussion

3.1. FTIR, NMR and ESI-MS characterizations of Ni(II)-SP Schiff base compound

The physical and chemical properties of the as-synthesized salphen ligand coordinated to nickel(II) metal centre with ethyl piperidine side chain [Ni(II)-SP] have been characterized based on FTIR, NMR and ESI-MS analyses. The addition of ethyl piperidine side chain is known for exhibiting hydrophilic characteristic of the resultant Schiff base metal salphen complex, whereby it will be protonated at ~ pH 7.0 and that enhances its DNA binding affinity [15,20]. The yield was 72% and appeared as brownish orange powder of Ni(II)-SP complex. Characterization of the Ni(II)-SP compound using ^{1}H NMR exhibited 11 proton peaks (Fig. A1). There are proton signals at 4.05 ppm (2H, $–CH_2$) and 2.78 ppm (2H,-CH_2), which represent the presence of alkyl groups, whilst the peaks proton signals at 2.55 ppm (2H), 1.63 ppm (1H) and 1.47 ppm (2H) correspond to the piperidine side chain of the symmetrical salphen ligand. ^{13}C NMR spectrum in Fig. A2 in the Supplementary Data portrayed all the carbon peaks for Ni(II)-SP compound. The alkylamine substituent is indicated by the alkyl carbon peaks at 66.46 ppm and 57.97 ppm, and the carbon signals of piperidine are shown at 55.04 ppm, 25.85 ppm and 24.11 ppm. Assignment of protons were further confirmed with 2D NMR (i.e. COSY and HMQC). The 2D-COSY NMR spectrum of the metal salphen label in Fig. A3 in the Supplementary Data shows the correlation between adjacent protons, whereby proton H1 is neighbouring with proton H2, whilst proton H7 is coupled with proton H8, and proton H9 is coupled with proton H10.2D-HMQC NMR (Fig. A4), on the other hand, indicates the interaction between carbon and proton. Based on 2D NMR spectrum that results from the HMQC experiment, it is noticed to be consistent with the carbon and hydrogen as assigned in 1D NMR (Fig. A1 and Fig. A2). The FTIR spectrum of Ni(II)-SP Schiff base ligand (Fig. A5) shows absorption bands at 2929.6 cm^{-1} and 2852.9 cm^{-1} which indicate the alkyl functional groups of C–H_2 and C–H. There are also absorption bands at 1600.3 cm^{-1}, 1526.5 cm^{-1}, 1203.0 cm^{-1} and 1122.9 cm^{-1} correspond to HC═N, C═C, C–N and C–O functional groups, respectively. The mass spectrum of the metal salphen compound in Fig. A6 in the Supplementary Data shows the molecular ion (M^+) peak at *m/z* 627.23 a.m.u., which is consistent with the theoretical molecular weight of $C_{20}H_{14}N_2NiO_4$ at 627.4 g mol^{-1}.

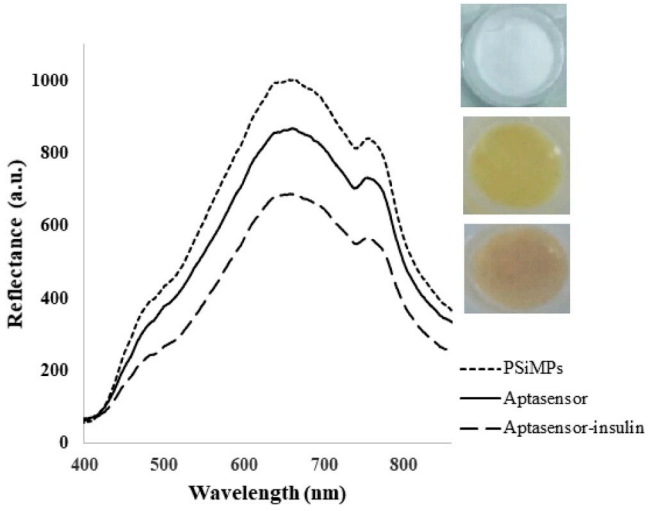

Fig. 2. Reflectance intensities of PSiMPs and aptasensor before and after addition of 1 mM metal complexes and 200 μIU mL^{-1} bovine pancreas insulin. The inset shows the visual colour change of the aptasensor from yellow to brownish orange upon immobilized IGA3-Ni(II)-SP complex bound with insulin. (For interpretation of the references to colour in this figure legend, the reader is referred to the Web version of this article.)

3.2. Characterization of aminated porous silica particles

Fig. A7 in the Supplementary Data exhibits the FESEM image of aminated PSiMPs prepared from a miniemulsion polymerization method. The FESEM micrograph shows a coral-like and porous structure of the silica microparticles with a mean diameter of 142.9 nm. The large surface area of the aminated porous microsilica would provide high binding capacity immobilization sites for high loading of DNA aptamers via glutaraldehyde cross-linking procedure [21]. The XRD spectrum of the as-synthesized aminated PSiMPs in Fig. A8 in the Supplementary Data demonstrating an amorphous peak with an equivalent Bragg angle at $2\theta = 21.8^{\circ}$ was registered.

3.3. Reflectance characterization of the insulin aptasensor based on metal salphen label

Fig. 2 illustrates the reflectance response of PSiMPs and DNA aptamer biosensor before and after binding with insulin. In view of the amine functionalized porous microsilica appeared as white microparticles and that it reflected highest light intensity at maximum reflectance wavelength of 656 nm. Glutaraldehyde is a homobifunctional crosslinker containing an aldehyde residue at both ends of a 5-carbon alkane chain. Its primary reactivity is toward amine groups to form a Schiff base. The short chain length of 5 backbone carbon atoms allow the glutaraldehyde bifunctional linker to stand more upright compared to its chain length exceeding 14, which adopts bending conformation. The short chain linker would tilt or bend away from each other without overlapping, causing their tails to be splayed apart, and leading to one end of aldehyde residue binds to amino group of silica substrate, and another end free to conjugate with amino-substituted DNA aptamer [22]. IGA3 aptamer conjugated PSiMPs via glutaraldehyde cross-linking, however, attenuated the reflectance intensity as a result of chemical binding reaction between aldehyde functional groups of glutaraldehyde and amine functional groups of PSiMPs and IGA3 aptamers that formed the Schiff base links i.e. RR'C=NR", R"≠H [23], and exhibited pale yellow colouration of the aptasensor micro surface. As the square planar salphen label bound to the G-quartet plane of folded single strand IGA3 aptamer via π-π stacking interaction, it formed an immobilized IGA3-Ni(II)SP complex, and gave a bright yellow colouration to the aptasensor. Upon binding with insulin, the dye-labeled aptasensor demonstrated a colour change from yellow to brownish orange, and considerably attenuated the aptasensor reflectance signal at 656 nm.

3.4. Effect of buffer solution and pH on the optical aptasensor response

The type of buffer used in the preparation of IGA3 aptamer solution including aptamer binding buffer is important to maintain the physical stability of aptamer and its affinity towards target substance [24]. Based on the results shown in Fig. A9 in the Supplementary Data, the use of TKN buffer as aptamer binding buffer gave the highest reflectance signal in the detection of 50 μIU mL^{-1} insulin at pH 7.4 compared to when PBS and NPS buffers were used. This was ascribed to the presence of K^+ and Na^+ ions in TKN buffer, which facilitated to maintain the integrity of Ni(II)-SP-labeled IGA3 G-quadruplex folded structure, and allowed the immobilized aptamer to bind to insulin with high specificity. This result is in agreement with Yoshida et al. [16] in their solution binding assay using different DNA aptamers against insulin in TKN buffer by fluorescence polarization measurement.

pH of the aptamer binding buffer would also give an enormous impact on the degree of aptamer binding specificity as aptamer binds by complementary nucleic acid base pairing [25], i.e. via hydrogen bonding between complementary bases that hold the single strand IGA3 nucleic acids together to form a tertiary structure of anti-parallel G-quadruplex DNA, which binds insulin selectively to form a stable Ni(II)-SP-labeled IGA3 aptamer-insulin complex. And, the ability to form hydrogen bonds between complementary nucleotides is very much dependent on the pH environment. As Fig. A10 indicates, in acidic conditions, sugar phosphate backbone of nucleic acid was undergoing protonation reaction, and consequently reducing the solubility of aptamer molecules in aqueous surrounding, thereby affecting the configuration of immobilized aptamer G-quartet structure, and decreasing the binding reaction rate between IGA3 and insulin. Aptamer-insulin recognition in alkaline pH, on the other hand, did not show any remarkable enhancement in reflectance signal due to basic buffer solution has broken up weak hydrogen bonds between nucleobases, and resulted in denaturation of the entire immobilized aptamer. Optimum aptasensor reflectance response was attained at pH 7.4 as it favoured the formation of G4 structure by the G-rich sequence of aptamer, and G-quadruplex was formed by stacking of G-quartets. Therefore, optimum pH at pH 7.4 was employed in the following aptasensor optimization experiments for optimal aptamer function.

3.5. Dynamic linear range of the DNA aptamer biosensor

Fig. 3a represents the reflectance response curve of DNA aptamer biosensor in various insulin concentrations from 1 to 200 μIU mL^{-1} at pH 7.4 and 656 nm. The optical reflectance response of the aptasensor increased with the increasing of insulin concentration from 1 μIU mL^{-1} to 50 μIU mL^{-1} with Ni(II)-SP Schiff base label concentration was held constant at 1 mM. This was attributed to the increasing aptamer-insulin binding reaction rate as increasing the insulin concentration. However, the aptasensor optical response become horizontalized as the concentration of insulin increased above 50 μIU mL^{-1}. At this stage, the immobilized dye-labeled IGA3 has reached a saturation point. A linear calibration curve of the aptasensor was determined to be between 10 μIU mL^{-1} and 50 μIU mL^{-1} insulin with a coefficient of determination (R^2) was obtained at $R^2 = 0.9757$, which signifies a linear relationship between reflectance signal and insulin concentration has achieved. The linearity of the calibration curve of reflectance insulin aptasensor from 10 to 50 μIU mL^{-1} was assessed by using residual plot as shown in Fig. A11 (see Supplementary Data). By plotting residuals can help one to determine lack of fit or uneven variance. For an ideal linear regression line, the residuals should be centered around zero throughout the calibration range, and free of any patterns appear as a random scatter of points. The residual plot shows that the distribution of residuals

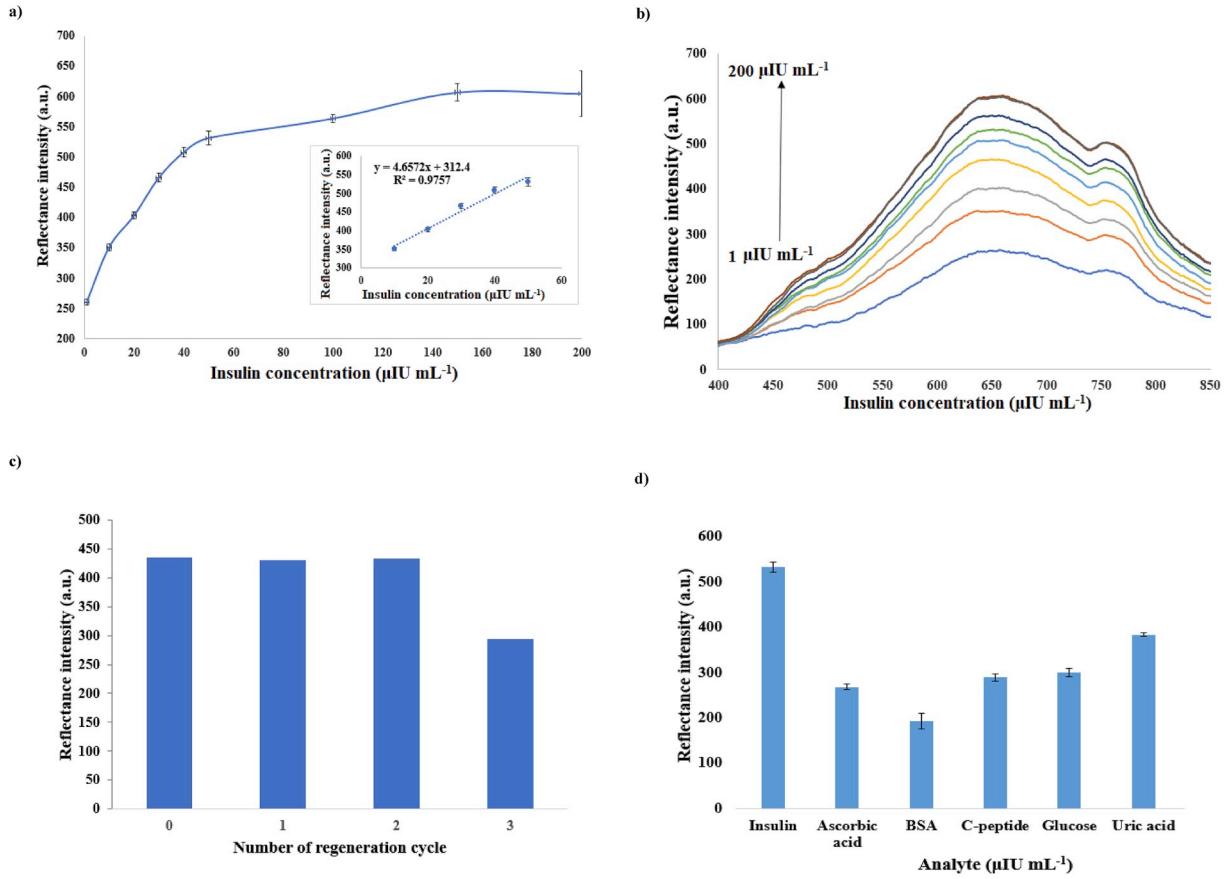

Fig. 3. (a) Response curve of the optical aptasensor towards the detection of different insulin concentrations from 1 μIU mL^{-1} to 200 μIU mL^{-1} at pH 7.4 and 656 nm. The inset shows the linear calibration range of the aptasensor between 10 μIU mL^{-1} and 50 μIU mL^{-1} insulin (n = 3). (b) The reflectance spectra of the DNA aptamer biosensor towards insulin in the concentration range of 1–200 μIU mL^{-1} at pH 7.4. (c) Reversibility performance of insulin aptasensor using 0.1 M NaOH regeneration solution and (d) Selectivity of reflectance insulin aptasensor using ascorbic acid, BSA, C-reactive peptide, D+ glucose monohydrate and uric acid prepared at physiological concentrations normally present in human blood serum in TKN buffer at pH 7.4 (n = 3).

exhibited a non-linear behaviour, and the response factor plot (Fig. A12 in the Supplementary Data) revealed the sensitivity declined when concentration of calibration standards was increased [26]. The limit of detection (LOD) of insulin aptasensor, which corresponds to the average of blank aptasensor reflectance response plus three standard deviations of blank aptasensor response was estimated at 3.71 μIU mL^{-1} insulin. The reflectance spectra of the DNA aptamer biosensor towards insulin in the concentration range of 1–200 μIU mL^{-1} is depicted in Fig. 3b.

3.6. Regeneration and selectivity of the insulin aptasensor

Regeneration of optical insulin aptasensor based on Ni(II)-SP-labeled IGA3 G-quadruplex immobilized on the PSiMPs has been investigated using 0.1 M NaOH regeneration solution. As can be seen in Fig. 3c, the aptasensor was capable of maintaining its initial response for optical assessment of 50 μIU mL^{-1} insulin after regenerated twice with 0.1 M NaOH, and its reflectance intensity drastically decreased by 32% after the third regeneration cycle with 0.1 M NaOH regeneration solution. This can be explained by the fact that the hydrogen bonds between complementary base pairs within IGA3 aptamer single strand loop have been broken up by 0.1 M NaOH, and resulted in unfolding of anti-parallel G-quadruplex DNA [27–29]. As G-quadruplex structure collapsed into linear single nucleic acid strand, the insulin binding sites become no longer available. Hence, it can be deduced that the Ni(II)-SP-labeled aptasensor can be reused for two consecutive assays of insulin.

Selectivity is an important parameter for specificity performance evaluation of the fabricated insulin aptasensor. Fig. 3d shows the selectivity performance of the developed reflectance aptasensor based on SSM method using several substances normally present in human blood serum, e.g. ascorbic acid, BSA, C-reactive peptide, D+ glucose monohydrate and uric acid. The optical aptasensor exhibited a maximum reflectance response towards insulin (relative intensity = 100%) detection, whereas other substances, such as ascorbic acid (relative intensity = 50%), BSA (relative intensity = 36%), C-reactive peptide (relative intensity = 54%), D+ glucose monohydrate (relative intensity = 56%) and uric acid (relative intensity = 72%) showed significant deviation of more than 25% decline in the reflectance response compared to the target insulin at 656 nm. This suggests good selectivity of the aptasensor based on IGA3 aptamer-immobilized porous microsilica towards insulin detection. And, optical reflectance insulin sensing based on strong π-π interaction between aromatic carbons of folded single strand IGA3 aptamer and planar aromatic groups of Ni(II)-SP is established.

3.7. Response time and shelf life of the reflectance insulin aptasensor

Fig. 4a shows the response time trending of optical aptasensor during determination of 50 μIU mL^{-1} insulin in TKN buffer (pH 7.4) with the presence of 1 mM Ni(II)-SP metal salphen ligand. The reflectance response of aptasensor was observed to gradually increase with time from 10 min to 40 min due to increasing Ni(II)-SP-labeled IGA3-insulin binding reaction rate. No obvious increment of reflectance signal after 40 min of reaction time as the aptamer-insulin binding reaction has reached a plateau state. Therefore, the aptasensor reaction time with insulin was maintained at 40 min before optical reflectance

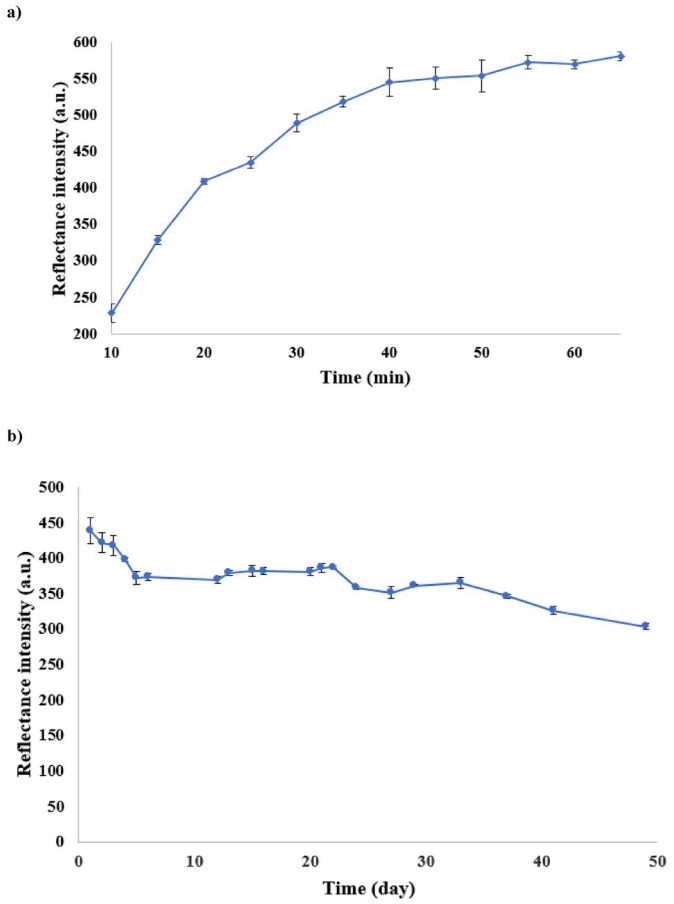

Fig. 4. a) Response time trending of optical DNA aptamer biosensor for the determination of 50 μIU mL^{-1} insulin for 60 min using 1 mM Ni(II)-SP Schiff base label (n = 3), and b) long term stability profile of the reflectance insulin aptasensor for a 50-day storage period at 25 °C, and detection of insulin was performed using 50 μIU mL^{-1} insulin in TKN buffer (pH 7.4) containing 1 mM Ni(II)-SP metal salphen ligand (n = 3).

reading was taken at the working wavelength of 656 nm in the subsequence analytical studies.

The long term stability performance of the developed optical insulin aptasensor is demonstrated in Fig. 4b. The operational stability of the aptasensor response in terms of optical reflectance response towards sensing of 50 μIU mL^{-1} insulin in TKN buffer (pH 7.4) containing 1 mM Ni(II)-SP metal salphen ligand was perceived to be capable of retaining its maximum level for the first five days of the experimental period, after which the aptasensor response dropped to 85.2% of its original response on day-6 of storage at room temperature, and the DNA aptamer biosensor response remained stable until day-24 before a substantial decline to about 69.2% of its initial response was occurred on day-50. The long shelf life of the aptasensor, i.e. > 3 weeks implies that the imine covalent bond formed between amine functional groups of IGA3 aptamer and aldehyde functional groups of glutaraldehyde [30,31] could render high stability of the resulting insulin aptasensor. Nevertheless, a considerable decline of the optical aptasensor response after 24 days of storage period may be attributed to the degradation of immobilized DNA aptamer, whereby the insulin binding sites of aptamer become distorted, and hindered its specific binding with insulin.

3.8. Comparison between developed optical insulin aptasensor and other reported insulin sensors

Table 1 summarizes the analytical performance of the previously reported electrochemical sensor/biosensor compared to the developed

Table 1
The performance comparison between the proposed DNA aptamer biosensor and other reported sensor for insulin quantification.

Receptor and immobilization matrix	Transducer	Linear range (μIU mL^{-1})	LOD (μIU mL^{-1})	Response time (min)	Reference
Ni(II)-SP-labeled IGA3 immobilized on PSiMPs	Fiber optic reflectance spectrophotometer	10.00–50.00	3.71	40	This work
IGA3 and Au-o-phenylenediamine polymer modified pencil graphite electrode	Electrochemical EIS	14.40×10^{1}–14.40×10^{4}	3.89	90	Ensafi et al. [25]
CuS–SiO2-labeled Ab_2 conjugated C–TiO2/CdS	PEC	25.00×10^{-4}-12.50×10^{2}	75.00×10^{-5}	40	Wang et al. [8]
IGA3-hemin complex immobilized gold electrode	Electrochemical CV	14.40×10^{4}–71.99×10^{4}	14.40×10^{4}	30	Kubo & Eguchi [6]
rGO modified glassy carbon electrode	Electrochemical CV and hydrodynamic amperometry	14.40×10^{3}–14.40×10^{4}	71.99×10^{2}	–	Noorbaksh et al. [7]

Table 2
Comparison of the proposed DNA aptamer biosensor with currently available commercial technologies for insulin detection.

Method	ELISA	RIA	IRMA	Developed optical aptasensor
Sensitivity (μIU mL^{-1})	0.170	2.715	0.200	3.710
Linear range (μIU mL^{-1})	5.1–250.0	2.0–200.0	0.0–500.0	10.0–50.0
Response time	45 min	Overnight	2 h	40 min
Simplicity	Need an expert	Need an expert	Need an expert	User-friendly
Cost	High	High	High	Low
Amount of sample (μL)	50	100	50	24

Table 3
Recovery performance of the optical DNA aptamer biosensor for insulin detection in commercial insulin sample ($n = 3$).

Sample	Spiked bovine pancreas insulin concentration (μIU mL^{-1})	Insulin concentration detected by aptasensor (μIU mL^{-1})	Recovery (%)
1	20	21.54 ± 0.80	107.7
2	30	30.47 ± 3.09	101.6
3	40	42.29 ± 1.59	105.7
4	50	50.39 ± 1.64	100.8

optical aptasensor for insulin detection. Thus far, no one has reported any optical biosensor approaches for sensing of insulin, therefore we believe this is the first report of optical aptasensor-based sensing platform for quantitative assessment of insulin. Previously reported electrochemical biosensor methods could detect insulin at high sensitivity, for instance, IGA3 and gold nanoparticles (Au)-decorated poly-orthophenylene diamine modified pencil graphite electrode based on electrochemical impedance spectroscopy (EIS) [25], and CuS–SiO_2-labeled secondary antibody (Ab_2) conjugated CdS sensitized carbon doped titanium dioxide (C–TiO2/CdS) by means of photoelectrochemical (PEC) immunosensor [8]. Anyhow, they required long insulin assay time and the electrodes sustained poor long term stability. Electrochemical insulin sensing using aptamer-immobilized gold electrode based on peroxidase activity of IGA3 with hemin by electrochemical cyclic voltammetry (CV) study, and reduced graphene oxide modified glassy carbon electrode (GCE) by electrochemical CV and hydrodynamic amperometry [7], however, were giving linear detection range of insulin at high concentration levels i.e. above normal human fasting insulin range. This impedes direct detection of insulin, and dilution step is necessary before the process of quantifying insulin concentration can be carried out. Furthermore, the use of GCE electrode sustained from electrode deactivation during successive sweeps, which was attributed to the electrode surface fouling with accumulation of insulin oxidation products.

Table 2 shows the comparison between the proposed optical aptasensor and commercial methods for insulin detection. Overall, the developed aptasensor shows excellent performance in terms of rapid detection (40 min) compared to ELISA, RIA and IRMA techniques, which require 45 min, overnight and 2 h, respectively. Besides, the proposed aptasensor offers a more user-friendly approach of insulin monitoring, whilst ELISA, RIA and IRMA demanding technical expertise on the insulin testing. In addition, those commercial technologies involved huge and complex instruments, radioactive reagent and high operational costs that restrict their application for real-time monitoring purposes.

3.9. Analytical application of the optical aptasensor

Commercial insulin injection i.e. insulin aspart from Novo Nordisk was used to verify the practical application of the proposed reflectance aptasensor. Insulin aspart is an analogue of human insulin with B28 amino acid proline substitution with aspartic acid. Its non-medicinal ingredients comprised of disodium phosphate dihydrate, glycerol, phenol and hydrochloric acid. Analytical application of the optical aptasensor via recovery of spiked standard bovine pancreas insulin within the linear concentration range of aptasensor in diluted commercial insulin samples showed recovery percentages in the range of 100.8–107.1% (Table 3), which is acceptable to consider that the developed aptasensor is reliable to be applied for practical assessment of insulin concentration.

3.10. Aptasensor versus ELISA kit for determination of insulin in human blood sample

Optical detection of insulin in human serum samples with the proposed aptasensor were carried out in triplicate for blood samples collected from three healthy volunteers under informed consent, and compared with ELISA reference method using BIOMATIK Human INS (Insulin) ELISA Kit. Dependent samples *t*-test or paired *t*-test was applied to statistically compare the results obtained with ELISA, the gold standard assay for measuring insulin and reflectometric aptasensor. Based on the results tabulated in Table 4, the *t*-values for a 95 confidence ($p = 0.05$) interval estimation with 4° of freedom were obtained to be smaller than the critical value at $t_4 = 2.776$. This suggests no significant difference between the results acquired by both ELISA and DNA aptamer biosensor and that the two methods are comparable at 95% confidence level, whereby the reflectometric aptasensor shows high potential to offer as an alternative real-time monitoring solution for clinical diagnostic application.

4. Conclusions

The optical aptasensor developed by grafting of aminated IGA3 aptamer to amine-modified PSiMPs by glutaraldehyde crosslinking has been successfully characterized for optical reflectance measurement of insulin based on colour change of the aptasensor, ascribed to the yellowish Ni(II)-SP Schiff base metal salphen complex, which acted as an immobilized optical label to the insulin binding DNA aptamer by π–π stacking interactions between aromatic rings of IGA3 G-quadruplex DNA aptamer and Ni(II)-SP label. When insulin was introduced, and bound to the immobilized Ni(II)-SP-labeled IGA3 DNA aptamer, a remarkable decline in the reflectance signal at 656 nm due to brownish

Table 4
Validation of optical aptasensor with commercial ELISA kit for insulin determination in human blood samples ($n = 3$).

Sample type	Sample	Insulin concentration determined by aptasensor (μIU/mL)	Insulin concentration determined by ELISA (μIU/mL)	*t*-value
Blood (serum)	1	17.55 ± 3.3100	17.29 ± 0.0049	0.136
	2	25.48 ± 2.5000	25.88 ± 0.0056	0.277
	3	6.23 ± 1.9700	8.11 ± 0.0064	1.650

$t4 = 2.776$ ($p = 0.05$)

orange aptamer-insulin complex was formed on the aptasensor micro surface. The reflectance aptasensor shows great promise for the detection of insulin simply by observing the colour change of aptasensor. Thus, achieving a convenient and facile strategy for insulin monitoring. The proposed optical aptasensor exhibited high selectivity and rapid response (i.e. 40 min) compared to traditional ELISA, RIA, IRMA and HPLC routine methods for quantitative insulin detection. The aptasensor is regenerable using 0.1 M NaOH and can be reused for twice for assay of insulin.

Acknowledgements

This work was supported by National University of Malaysia (UKM) via Research University Grant [GUP-2018-156].

Appendix A. Supplementary data

Supplementary data to this article can be found online at https://doi.org/10.1016/j.talanta.2019.120321.

References

[1] G. Wilcox, Insulin and insulin resistance, Clin. Biochem. Rev. 26 (2003) 19–39.
[2] S. Buppajarntham, Insulin, https://emedicine.medscape.com/article/2089224-overview, (2014) accessed: October 2018.
[3] World Health Organization, Definition, Diagnosis and Classification of Diabetes Mellitus and its Complications, (1999).
[4] A. Najjar, M. Alawi, N. Abuheshmeh, A. Sallam, A rapid, isocratic HPLC method for determination of insulin and its degradation product, Adv. Pharm. (2014) 1–6.
[5] A. Kaur, N. Verma, Electrochemical biosensor for monitoring insulin in normal individuals and diabetic mellitus patients, Eur. J. Exp. Biol. 2 (2012) 389–395.
[6] I. Kubo, T. Eguchi, Study on electrochemical insulin sensing utilizing a DNA aptamer-immobilized gold electrode, Materials 8 (2015) 4710–4719.
[7] A. Noorbakhsh, A.I.K. Alnajar, Antifouling properties of reduced graphene oxide nanosheets for highly sensitive determination of insulin, Microchem. J. 129 (2016) 310–317.
[8] X. Wang, P. Gao, T. Yan, R. Li, R. Xu, Y. Zhang, B. Du, Q. Wei, Ultrasensitive photoelectrochemical immunosensor for insulin detection based on dual inhibition effect of CuS-SiO2 composite on CdS sensitized C-TiO_2, Sens. Actuators B Chem. 258 (2018) 1–9.
[9] A.K. Yagati, Y. Choi, J. Park, J.W. Choi, H.S. Jun, S. Cho, Silver nanoflower-reduced graphene oxide composite based micro-disk electrode for insulin detection in serum, Biosens. Bioelectron. 80 (2016) 307–314.
[10] M. Jarczewska, L. Gorski, E. Malinowska, Electrochemical aptamer-based biosensors as potential tools for clinical diagnostics, Anal. Methods 8 (2016) 3861–3877.
[11] S. Song, L. Wang, J. Li, C. Fan, J. Zhao, Aptamer-based biosensors, Trac. Trends Anal. Chem. 27 (2008) 108–117.
[12] Q. Cao, Y. Li, E. Freisinger, P.Z. Qin, R.K.O. Sigel, Z. Mao, G-quadruplex DNA targeted metal complexes acting as potential anticancer drugs, Inorg. Chem. Front. 4 (2017) 10–32.
[13] B.J. Pages, D.L. Ang, E.P. Wright, J.R. Aldrich-Wright, Metal complex interactions with DNA, Dalton Trans. 44 (2015) 3505–3526.
[14] S.N. Georgiades, A.K. Nurul Huda, K. Suntharalingam, R. Vilar, Interaction of metal complexes with G-quadruplex DNA, Angew Chem. Int. Ed. Engl. 49 (2010) 4020–4034.
[15] A.K. Nurul Huda, O. Mendoza, A. Shivalingam, A.J. Thompson, S. Ghosh, M.K. Kuimova, R. Vilar, Salphen metal complexes as tunable G-quadruplex binders and optical probes, RSC Adv. 4 (2014) 3355–3363 2014.
[16] W. Yoshida, E. Mochizuki, M. Takase, H. Hasegawa, Y. Morita, H. Yamazaki, K. Sode, K. Ikebukuro, Selection of DNA aptamers against insulin and construction of an aptameric enzyme subunit for insulin sensing, Biosens. Bioelectron. 24 (2009) 1116–1120.
[17] A. Arola-Arnal, J. Benet-Buchholz, S. Neidle, R. Vilar, Effects of metal coordination geometry on stabilization of human telomeric quadruplex DNA by square-planar and square-pyramidal metal complexes, Inorg. Chem. 47 (2008) 11910–11919.
[18] N.H. Campbell, A.K. Nurul Huda, G.N. Parkinson, M. Gunaratnam, V. Petruccit, A.K. Todd, R. Vilar, S. Neidle, Molecular basis of structure–activity relationships between salphen metal complexes and human telomeric DNA quadruplexes, J. Med. Chem. 55 (2012) 209–222.
[19] M. Alqasaimeh, Y.H. Lee, A. Musa, A.S. Santhana Raj, L.L. Tan, A large response range reflectometric urea biosensor made from silica-gel nanoparticles, Sensors 14 (2014) 13186–13209.
[20] C.Q. Zhou, T.C. Liao, Z.Q. Li, J. Gonzalez-Garcia, M. Reynolds, M. Zou, R. Vilar, Dinickel–salphen complexes as binders of human telomeric dimeric G-quadruplexes, Chem. Eur J. 23 (2017) 4713–4722.
[21] A. Beganskiene, V. Sirutkaitis, M. Kurtinaitiene, R. Juskenas, A. Kareiva, FTIR, TEM and NMR investigations of stöber silica nanoparticles, Mater. Sci.-Medzg. 4 (2004) 287–289.
[22] J.E. Black, A.Z. Summers, C.R. Iacovella, P.T. Cummings, C. McCabe, Investigation of the impact of cross-polymerization on the structural and frictional properties of alkylsilane monolayers using molecular simulation, Nanomaterials 9 (2019) 639–659.
[23] S. Nagarajan, Z. Li, V. Marchi-Artzner, F. Grasset, Y. Zhang, Imaging gap junctions with silica-coated upconversion nanoparticles, Med. Biol. Eng. Comput. 48 (2010) 1033–1041.
[24] M. Ilgu, M. Nilsen-Hamilton, Aptamers in analytics, Analyst 141 (2016) 1551–1568.
[25] A.A. Ensafi, E. Khoddami, B. Rezaei, Aptamer@Au-o-phenylenediamine modified pencil graphite electrode: a new selective electrochemical impedance biosensor for the determination of insulin, Colloids Surfaces B Biointerfaces 159 (2017) 47–53.
[26] J.M. Juradoa, A. Alcázara, R. Muñiz-Valenciab, S.G. Ceballos-Magañac, F. Rapos, Some practical considerations for linearity assessment of calibration curves as function of concentration levels according to the fitness-for-purpose approach, Talanta 172 (2017) 221–229.
[27] A.C. Connor, K.A. Frederick, E.J. Morgan, L.B. McGrown, Insulin capture by an insulin-linked polymorphic region G-quadruplex DNA oligonucleotide, J. Am. Chem. Soc. 128 (2006) 4986–4991.
[28] W. Yoshida, T. Saito, T. Yokoyama, S. Ferri, K. Ikebukuro, Aptamer selection based on G4-forming promoter region, PLoS One 8 (2013) e65497.
[29] L.H. Lauridsen, H.A. Shamaileh, S.L. Edwards, E. Taran, R.N. Veedu, Rapid one-step selection method for generating nucleic acid aptamers: development of a DNA aptamer against alpha-bungarotoxin, PLoS One 7 (2012) e41702.
[30] L. Betancor, F. Lopez-Gallego, A. Hidalgo, N. Alonso-Morales, G.D.C. Mateo, R. Fernández-Lafuente, J.M. Guisan, Different mechanisms of protein immobilization on glutaraldehyde activated supports: effect of support activation and immobilization conditions, Enzym. Microb. Technol. 39 (2006) 877–882.
[31] P. Monsan, Optimization of glutaraldehyde activation of a support for enzyme immobilization, J. Mol. Catal. 3 (1978) 371–384.